Light Scattering by Ice Clouds in the Visible and Infrared: A Theoretical Study

KUO-NAN LIOU

Institute for Space Studies, Goddard Space Flight Center, NASA, New York, N. Y. 10025

(Manuscript received 9 November 1971, in revised form 30 December 1971)

ABSTRACT

Computations of the intensity and linear polarization for single scattering by ice clouds have been made based on the assumption that the particles in ice clouds can be approximated by long circular cylinders which are allowed to be polydispersive as well as arbitrarily oriented in space. The results of two models of optically thin ice clouds are presented and compared with those for polydisperse ice spheres. The two models for ice cylinders are assumed to be either uniformly or randomly oriented in a horizontal plane. Four different wavelengths, 0.7, 3, 3.5 and 6.05 μ, are employed in the light scattering computations.

It is found that, compared to ice spheres, long ice cylinders scatter more light in the region with scattering angles near 90°, at the expense of scattering in both the forward and backward directions. The glory and cloudbows, which occur in light scattered by spherical particles, are either lost (the glory) or largely reduced and distorted (the cloudbows) in the case of cylinders. It is probable that for more irregular particles the cloudbows would also disappear. These differences in scattering by spherical and non-spherical scatterers therefore provide useful information for the differentiation between the ice and liquid phase of cloud particles.

The light scattering computations performed for ice cylinders in this paper represent a new theoretical approach in an attempt to understand the radiation scattered by ice crystals. Hence, results of the angular scattering patterns for ice cylinders could be of use in the evaluation of the transfer of visible or infrared radiation through thick ice clouds, especially cirrus.

1. Introduction

There are two important problems that require detailed knowledge of the phase function (which indicates the distribution of the scattered energy) of ice crystals in the visible and infrared regions: first, the evaluation of the transfer of visible and infrared (IR) radiation through ice clouds, especially cirrus, to understand the effects of clouds on the atmospheric radiation balance and the atmospheric visibility; and second, the inference of the composition (phase, size, dispersion, water content, etc.) of clouds by means of remote sensing techniques.

With regard to the above two aspects of the problem, several theoretical investigations have recently been reported. Houghton and Hunt (1971) have claimed that the thickness and particle size of ice clouds may be detected from their emission in the far IR. Hansen and Pollack (1970) and Twomey (1971) have proposed that ice and water clouds could be distinguished by their scattered radiation in the near IR based on the reflectance calculations. The former authors have also computed the reflectivity of ice clouds in the near IR regions to derive the size of cloud particles and the optical thickness. Harris (1971) has suggested that ice and water clouds may be discriminated by laser beam scattering based on calculations for the two phases at wavelengths where there is a marked difference in the refractive indices. Plass and Kattawar (1971) have evaluated the transfer of visible and IR radiation through ice clouds by employing a Monte Carlo method.

Among these interesting and important calculations, the understanding of the angular scattering dependence (or phase function) is obtained from Mie theory (1908) for *spheres*. The effects of *shapes* of ice crystals on scattered radiation seem to have been largely ignored. The significance of the shape effect on scattered radiation has been noted by radar meteorologists for sometime (see, e.g., Battan, 1959). Recently, Liou and Schotland (1971) have proposed a depolarization technique for distinguishing between ice and water clouds based on the principle that the backscattered radiation from water drops retains the polarization of the incident energy, while the scattered radiation from non-spherical ice crystals is partially depolarized. However, no quantitative values for scattering by ice crystals were given. Jacobowitz (1970, 1971) has evaluated the angular scattering patterns for infinite hexagonal cylinders by means of geometrical optics. Liou (unpublished) has also carried out some ray optics computations for ellipsoids. But effects of polarization were not considered in either case.

Ice clouds contain predominantly non-spherical crystals. While a great deal of research has been focused on the problems of scattering by spheres, there are practically no comprehensive theoretical studies for predicting the scattering of light by non-spherical

particles. The primary purpose of the present investigation is therefore to develop a theoretical approach to provide light scattering information for non-spherical scatterers.

In this study, we assume that ice clouds consist of *long* circular cylinders which are allowed to be polydispersive as well as arbitrarily oriented in space. Since the modeling of ice clouds in this paper is purely hypothetical, such cloud models may not resemble the ice crystals which occur in the terrestrial atmosphere. However, the results may be useful for an understanding of light scattering by, at least, certain types of ice crystals with shapes such as needles, columns, etc. The study of scattering by an individual cylinder is not new. Lord Rayleigh (1918) has solved the scattering by a homogeneous dielectric infinite cylinder at normal incidence. Wait (1955), Kerker (1969), and Liou (1972) have extended the solutions for oblique incidence. We have used the solutions of the scattering coefficients and scattered intensities derived by Liou, who followed most of the procedures outlined by van de Hulst (1957) for calculations of the phase functions.

Following the discussions of the scattering geometry and the problem of orientation, we derive the phase functions, the scattering cross sections, and the linear polarization for an incident unpolarized light with ice cylinders either uniformly or randomly oriented in a horizontal plane. Numerical results are presented, discussed, and compared to those of polydisperse ice spheres. The Mie calculations for polydisperse spheres are the same as those previously reported by Liou and Hansen (1971).

2. Scattering geometry

In this section we briefly describe the geometry of light scattered by a cylinder and define some angles for the problem of orientation. Fig. 1 represents the geometry of light scattered by a long cylinder with an oblique incidence. In this figure, the Z axis of the cylindrical coordinate system is placed along the central axis of the cylinder. The angle between the incident ray and the negative Z axis is denoted as χ, while α is the complement angle of χ and is defined as the "oblique incident angle." The rectangular coordinate X axis is defined on the plane containing the incident ray and the Z axis. This plane contains the angles $\phi=0$ and $\phi=\pi$. Since a long cylinder whose length is much larger than its diameter is considered in this study, the scattered radiation is confined to the surface of a solid cone which forms an angle α with the X, Y plane.

Two cases of linear polarization for the incident beam are considered; one is when the electric field **E** vibrates parallel to the plane containing the incident ray and Z axis, while the other is when **E** vibrates perpendicular to this plane. From these two cases, arbitrary elliptically polarized scattered light may then be constructed by means of a linear superposition from the two solutions.

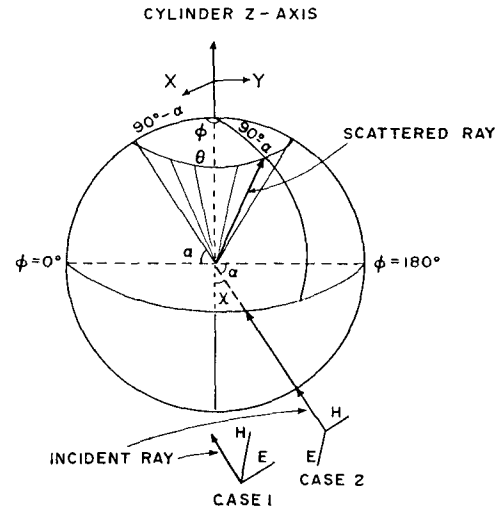

FIG. 1. Geometry of light scattered by an arbitrarily oriented long cylinder. The scattered radiation is confined to the surface of a solid cone. The figure also indicates the relationship between the scattering angle θ and the observation angle ϕ. Other symbols are explained in the text.

The scattering angle θ, which is defined as the angle between the directions of the incident wave and the scattered wave, can easily be obtained from the spherical geometry shown in Fig. 1 as follows:

$$\cos\theta=\sin^2\alpha+\cos^2\alpha\cos\phi. \tag{1}$$

We define $\phi(0,\pi)$ as an "observation angle" to distinguish if trom the scattering angle θ; ϕ and θ become equal only at normal incidence ($\alpha=0$) which is the case when the direct backscattering occurs.

Fig. 2 illustrates the orientation geometry of the cylinder. The X' axis is defined as a fixed vertical coordinate, while Z', Y' is a horizontal plane in which the Z' axis is located in the plane containing X' and the incident ray. To simplify the discussions below, let us put the cylinder on the Z', Y' horizontal plane. Now the angle between the incident ray and the Z axis of the cylinder is χ. Referring to this figure, we find the

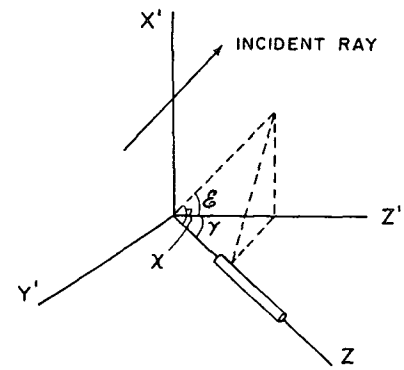

FIG. 2. Geometry of the orientation of a cylinder with respect to the incident ray. All symbols are defined in the text.

geometrical relationship

$$\cos\chi=\sin\alpha=\cos\mathcal{E}\cos\gamma, \tag{2}$$

where $\mathcal{E}$ is the angle between the incident ray and its projection on the Z' axis (or horizontal plane), and γ represents the angle which indicates the orientation of the cylinder in a horizontal plane. Hence, the angles $\mathcal{E}$ and γ with respect to the incident ray can be used to describe the orientation of the cylinder in the vertical and horizontal directions, respectively. We name $\mathcal{E}$ and γ the elevation and orientation angles, respectively, for the convenience of later discussion.

3. Theoretical considerations

For the purpose of formulating the intensity and linear polarization for single scattering by a sample of cylinders, let us consider the basic electromagnetic wave assuming that the incoming wave can be represented by the two electric field components E_l^i and E_r^i, which are parallel and perpendicular, respectively, to an arbitrary reference plane toward the direction of propagation of the incoming beam. Let us assume furthermore that the scattering event is a linear process, so that the outgoing wave can be represented by (van de Hulst, 1957)

$$\begin{bmatrix} E_l^s \\ E_r^s \end{bmatrix}=\begin{bmatrix} A_2 & A_3 \\ A_4 & A_1 \end{bmatrix}\begin{bmatrix} E_l^i \\ E_r^i \end{bmatrix}, \tag{3}$$

where E_l^s and E_r^s are the electric field components parallel and perpendicular, respectively, to a plane of reference toward the outgoing beam. From (3), it is easily understood that a polarized incident light is generally depolarized through the scattering process. In this study, we choose the plane containing the incoming beam and Z axis of the cylinder as the plane of reference for the incoming beam (see Fig. 1). We use case 1 and case 2 to indicate the incident electric field components vibrating parallel and perpendicular to this plane, respectively. The scattering amplitudes $A_j(j=1,2,3,4)$ at far field can be derived as follows for an arbitrarily oriented, infinitely long cylinder:

$$\left.\begin{aligned} A_2&=C\Big(b_{01}+2\sum_{n=1}^{\infty} b_{n1}\cos n\phi\Big)\\ A_3&=C\Big(2\sum_{n=1}^{\infty} a_{n1}\sin n\phi\Big)\end{aligned}\right\}\ \text{CASE 1} \tag{4}$$

$$\left.\begin{aligned} A_1&=C\Big(a_{02}+2\sum_{n=1}^{\infty} a_{n2}\cos n\phi\Big)\\ A_4&=C\Big(2\sum_{n=1}^{\infty} b_{n2}\sin n\phi\Big)\end{aligned}\right\}\ \text{CASE 2} \tag{5}$$

where

$$C=\left(\frac{2}{\pi kR}\right)^{\frac{1}{2}}\exp(i\omega t-ikR-i3\pi/4),$$

$$a_{n1}=-b_{n2},\quad \text{i.e.,}\quad A_3=-A_4,$$

k is the wavenumber, ω the circular frequency, $i=(-1)^{\frac{1}{2}}$, R represents the distance of the propagation of waves in a spherical coordinate, and ϕ is the observation angle mentioned in the last section. The formulas of the scattering coefficients a_n and b_n were first given by Wait (1955) for case 1, and later by Kerker (1969) in a matrix form. Recently, Liou (1972) has derived the values for a_n and b_n in forms more suitable for computer calculations. These coefficients involve Bessel functions of the first kind, Hankel function of the second kind and their first derivatives, and are functions of the refractive index n of the scattering medium and the size parameter x, which is the ratio of the circumference of the cylinder to the incident wavelength. Moreover, the scattering coefficients also depend on the values of the oblique incident angle α which is formed by the direction of the incident beam and the position of the cylinder. While the assumption is made that the cylinder is infinitely long, so that the waves can be treated as periodic along the cylindrical Z axis and a simple form of the incident field may be derived, the solutions for scattering coefficients, however, should be applied with rather good accuracy for a cylinder whose length is much larger than its diameter.

In order to obtain the phase function (or scattering diagram) which is a quantity indicating the angular distribution of the scattered energy, let us further define the so-called "intensity coefficients" i_j as

$$i_j=|A_j|^2\frac{\pi kR}{2},\quad j=1,2,3,4, \tag{6}$$

where i_j are dimensionless parameters which have meaning similar to i_1 and i_2 in the case of light scattering by spherical particles. It should be noted that i_3 and i_4 are depolarized components which arise because of the oblique incidence.

Now, let $\mathbf{P}$ be a four-by-four phase matrix with respect to the Stokes parameters (I,Q,U,V), and let P^{ij} represent the elements in the ith row and jth column, respectively. For an unpolarized incident light with Stokes parameters (1,0,0,0), the only two elements which associate with the scattered intensity and linear polarization are

$$P^{11}(\alpha,\phi;x)=\frac{2}{\pi kC_s}i^{11}(\alpha,\phi;x), \tag{7}$$

$$P^{21}(\alpha,\phi;x)=\frac{2}{\pi kC_s}i^{21}(\alpha,\phi;x), \tag{8}$$

where

$$i^{11}(\alpha,\phi;x)=\tfrac{1}{2}[(i_2+i_3)+(i_1+i_4)], \tag{9}$$

$$i^{21}(\alpha,\phi;x)=\tfrac{1}{2}[(i_2+i_3)-(i_1+i_4)]. \tag{10}$$

The arguments on the right-hand side of Eqs. (9) and (10) are neglected for simplicity, and C_s is a quantity

defined as follows: By integrating the scattered intensity over all observation angles ϕ and over a length l in the Z direction, we obtain the total scattered energy per unit time by a length l of a cylinder. The value by definition can be denoted as (lC_sI_0), where I_0 is the incident intensity, and C_s the cross section of scattering per unit length (van de Hulst, 1957). Physically, C_s may be described as an effective width in which the total amount of scattered light (without absorption) equals the amount of the incident on the length l with width C_s. Hence, the scattering cross section per unit length for an incident unpolarized light can be defined as

$$C_s(\alpha; x)=\frac{2}{\pi k}\int_0^{2\pi} i^{11}(\alpha,\phi; x)d\phi$$

$$=\frac{2}{k}\{|b_{01}|^2+|a_{02}|^2$$

$$+2\sum_{n=1}^{\infty}[|b_{n1}|^2+|a_{n1}|^2+|a_{n2}|^2+|b_{n2}|^2]\}. \quad (11)$$

By means of the above definition, the phase function P^{11} for a single cylinder has the property

$$\int_0^{2\pi} P^{11}(\alpha,\phi; x)d\phi=1. \quad (12)$$

It should be noted that the scattered light from a single cylinder is confined to the surface of a solid cone whose size depends upon the oblique incident angle α (see Fig. 1). So far we have only discussed the derivation of the phase function and scattering cross section for a single cylinder; we shall now extend the definitions for them for a sample of ice cylinders in a cloud. Jayaweera and Mason (1965) have studied the behavior of freely falling cylinders in viscous fluids and have found that if the ratio of diameter to length is less than unity, then the cylinders will fall with their long axes horizontally. In the studies of the shape and riming properties of ice crystals in natural clouds, Ono (1969) has also indicated that columnar ice crystals fall with their major axes parallel to the ground. Since long cylinders are considered in this theoretical investigation, we therefore assume that they fall with their long axes in a horizontal plane. For the purpose of the numerical experiments, two ice cloud models (Fig. 3) are considered and discussed below. It should be noted that the two ice cloud models are assumed to be optically thin so that the effects of multiple scattering may be neglected.

a. Polydisperse ice cylinders with uniform orientation in a horizontal plane (model 1)

In the following theoretical investigations of light scattering by a sample of long ice cylinders, we define "polydisperse" by means of the variations of the cylindrical cross-section radii. In this case all the ice cylinders, whose radii vary according to the distribution functions (which will be discussed in a later section), are supposed to have the same orientations in a horizontal plane. Intensity scattered by a single particle, as a function of the scattering angle, usually contains several interference maxima and minima which depend upon the size parameter as well as the oblique incident angle (if the particle is nonspherical). But by assuming the variations in the cylinder radii, most of the interference patterns of the scattered intensity may then be washed out. Here, we also assume that independent scattering holds for these cylinders with uniform orientation in a cloud, so that the scattered intensities from such cylinders can be added without regard to phase. (Although, strictly speaking, the assumption of independent scattering may not be applied to a sample of cylinders having the same orientations. However, the sticky coherence problem is not in the scope of this study, and it will not be discussed here.) Based upon the above assumptions, the phase elements for ice cylinders with uniform orientation may be defined as

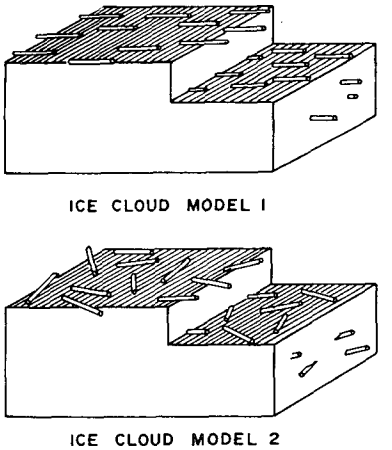

FIG. 3. Diagrams for the two ice cloud models. The upper part shows cylinders uniformly oriented in a horizontal plane, while the lower part denotes cylinders randomly oriented in a horizontal plane.

$$P^{m1}(\alpha,\phi)=\frac{2}{\pi k\beta_s}\int_{x_1}^{x_2} i^{m1}(\alpha,\phi; x)n(x)dx, \qquad m=1, 2, \quad (13)$$

where $n(x)$ represents the size distribution of the cylinders, x_1 and x_2 are the lower and upper limits of the size parameter, respectively, and the scattering cross section per unit length for a sample of cylinders is

$$\beta_s(\alpha)=\int_{x_1}^{x_2} C_s(\alpha; x)n(x)dx. \quad (14)$$

The scattered light from this cloud model is also confined to a solid cone. The geometry is essentially the same as that for a single cylinder.

b. Polydisperse ice cylinders with random orientation in a horizontal plane (model 2)

In this section we assume that every possible orientation of the cylinders in a horizontal plane is equally probable in the cloud and that the separation distance between the cylinders is much larger than the incident wavelength. Consequently, for such randomly oriented ice cylinders, the phases of the scattered electromagnetic waves are mostly averaged out so that the intensities scattered from each cylinder may then be added. For cylinders having random orientation, the scattered light is in all directions because the oblique incident angles α range from 0 to $\pi/2$. It is necessary and desirable to obtain the angular scattering patterns as functions of the scattering angle θ (rather than as functions of the observation angle ϕ), since the scattering cone from each randomly oriented cylinder is confined to different directions. In order to obtain the angular scattering patterns, all the possible intensities which scatter in the same directions (which can be represented by the scattering angles) have to be added together.

From the earlier discussion, the intensity coefficients i_j are found to be functions of the oblique incident angle α and the observation angle ϕ (as well as the size parameter x). The scattering geometry discussed in the previous section shows that the oblique incident angle can be expressed in terms of the orientation of the cylinder from Eq. (2) as

$$\alpha \equiv \alpha(\mathcal{E},\gamma). \tag{15}$$

Furthermore, from Eq. (1), we also find the relationship between the scattering angle and the observation angle to be

$$\phi \equiv \phi[\alpha(\mathcal{E},\gamma),\theta]. \tag{16}$$

From the above two equations, we can change uniquely the arguments of the intensity coefficients as follows:

$$i_j(\alpha,\phi;x) \equiv i_j(\mathcal{E},\gamma,\theta;x), \quad j=1,2,3,4. \tag{17}$$

Thus, the phase elements for a sample of ice cylinders randomly oriented in a horizontal plane may be obtained by integrating the orientation angle γ. Because the cylinder is symmetrical with respect to its central axis, integration over γ ranges only from 0 to $\pi/2$; thus,

$$P^{m1}(\mathcal{E},\theta) = \frac{2}{\pi k \beta_s} \int_0^{\pi/2} \int_{x_1}^{x_2} i^{m1}(\mathcal{E},\gamma,\theta;x) n(x) dx d\gamma, \quad m=1, 2. \tag{18}$$

For a given elevation angle $\mathcal{E}$, the scattered light is in all directions and is a function of the scattering angle θ only. To obtain the volume scattering cross section in this case, it is required to integrate the scattered intensity over the solid angle $d\Omega = \sin\theta d\theta d\varphi$. It is noted from the above formulations and reasonings that the scattered light from ice cylinders having random orientation in a horizontal plane is independent of the azimuth angle φ. Hence, we find

$$\beta_s(\mathcal{E}) = \frac{4}{k} \int_0^{\pi} \left\{ \int_0^{\pi/2} \int_{x_1}^{x_2} i^{11}(\mathcal{E},\gamma,\theta;x) n(x) dx d\gamma \right\} \sin\theta d\theta. \tag{19}$$

After the transformation of the angles, an analytic solution for $\beta_s(\mathcal{E})$ cannot be obtained. Thus, Eq. (19) must be numerically integrated. In view of the above definitions, the integral of the phase function P^{11} over the solid angle $d\Omega$ becomes unity. It is therefore possible to compare these results to those scattered by polydisperse spheres.

Finally, the linear polarization for an unpolarized incident light by means of the definitions of the phase elements in either models 1 or 2 yields

$$P = -\frac{Q}{I} = -\frac{P^{21}}{P^{11}}. \tag{20}$$

Some numerical results for these two cases are presented below.

4. Numerical results and discussions

The computations of the phase function and scattering cross section for cylinders involve the evaluation of the scattering coefficients a_n and b_n which consist of Bessel functions of the first kind and Hankel functions of the second kind. The Bessel functions were evaluated by employing the IBM scientific subroutines which were based on the technique developed by Abramowitz and Stegun (1965), and the arithmetic was carried out in double precision. The convergence criterion for Eqs. (4), (5) and (11) is set in such a way that the ratio of the absolute difference between the last two terms in the series to the last term is less than 10^{-10}. Hence the values for A_j/C and C_s are accurate within at least five decimal points. Below are some discussions of the numerical results. In the final subsection, we also carry out some comparisons of theoretical calculations with laboratory measurements.

a. Single cylinder

Since the numerical results for scattering by individual cylinders were discussed in detail in the author's previous paper, no graphs will be presented in this study. However, there are several interesting points worth being mentioned briefly. First, all the intensity coefficients i_j show interference maxima and minima which depend upon the size parameter as well as the incident angle. In addition, the depolarized components i_3 and i_4, which disappear only at normal incidence, have values comparable to i_1 and i_2 except at the very forward directions. Finally, the angular scattering patterns become rather simple and nearly symmetrical for large oblique incident angles.

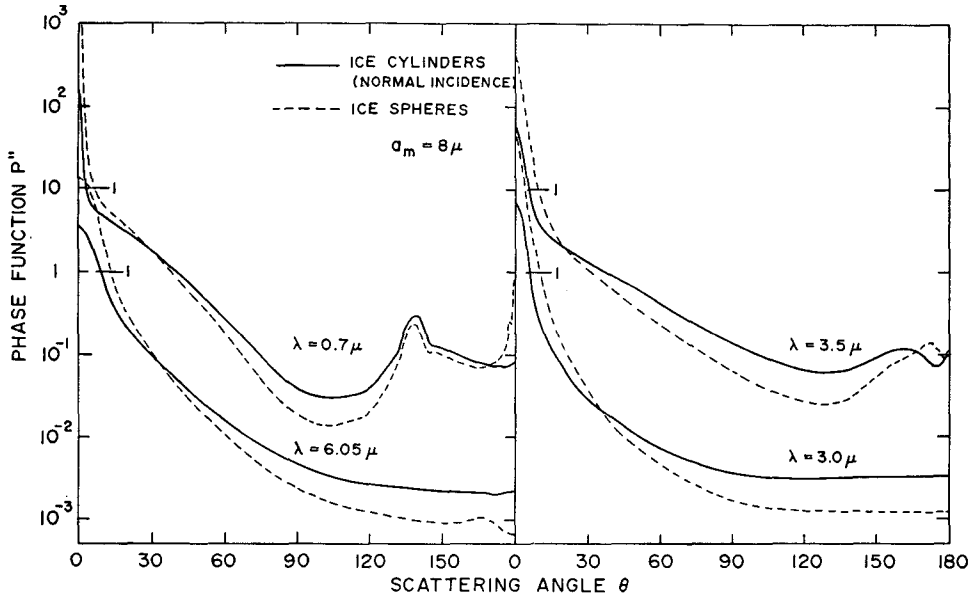

FIG. 4. Phase functions for uniformly oriented ice cylinders at normal incidence (solid lines) and for ice spheres (dotted lines) at wavelengths of 0.7, 3, 3.5 and 6.05 μ. The mode radius is 8 μ. The vertical scale applies to the lower curves, while the scale for the upper curves can be obtained by dividing by a factor of 10.

Although the solutions for scattering coefficients are derived based upon the assumption that the cylinder is infinitely long, they nevertheless should be applied with rather good accuracy to a finite cylinder whose length is much larger than its diameter. We can explain this physically by means of ray optics. If the diameter of the cylinder is much larger than the incident wavelength, then the incident rays can be localized. The rays undergoing reflection and/or refraction on the surface of the cylinder follow the well-known Snell's laws. And since the cylinder is very long, a ray that could possibly escape to the end of the cylinder would suffer a great number of internal reflections which contain negligible amounts of energy. Consequently, the scattered radiation is confined to the surface of a solid cone. As for Rayleigh types of cylinders in which their diameters are comparable to or smaller than the incident wavelength, Gary and Craven (1970) have experimentally shown that the light is also concentrated on the surface of a cone. Cooke and Kerker (1969) have measured the scattered radiation by individual finite long fibers using a wavelength of 0.546 μ. They have obtained excellent agreements of the linear polarization between measured data and theoretical computations for infinite cylinders. All the above experimental or physical arguments indicate that for scattering by a long cylinder (not necessarily infinitely long) the end effects are not important and can be neglected.

b. Uniformly oriented ice cylinders in a horizontal plane

We employ the modified Gamma function suggested and used by Deirmendjian (1964,1969) for the particle size distribution of clouds, i.e.,

$$n(a) \propto a^6 \exp(-6a/a_m), \tag{21}$$

where $n(a)$ represents the volume concentration of cylinder radius a, and a_m is the mode radius at which the distribution has its maximum. The Gaussian integration for the particle size was used in which the integrations over the size a were performed to an upper limit of $a_{\max}=2a_m$. The integration increments were chosen small enough to make the phase function as well as the linear polarization smooth (Dave, 1969). The calculations were performed at 91 observation angles, 0°(2°)180°. It should be mentioned that the primary purpose of integrating over the sizes is to average out the interference maxima and minima due to single particle effects, so that scattering features can be clearly shown. No claim is made in this paper that the above Gamma function represents a real size distribution for ice clouds in the atmosphere.

Besides the computations for ice cylinders, we have also calculated the light scattered by polydisperse ice spheres for comparison purposes. The programs for spheres are the same as those performed by Liou and Hansen (1971) in which the phase function is normalized to unity by

$$\int_{4\pi} P^{11}(\theta)d\Omega = 1, \tag{22}$$

where Ω is the solid angle and θ the scattering angle. In view of the definitions of scattering by ice cylinders and spheres, comparisons were made at the same mode

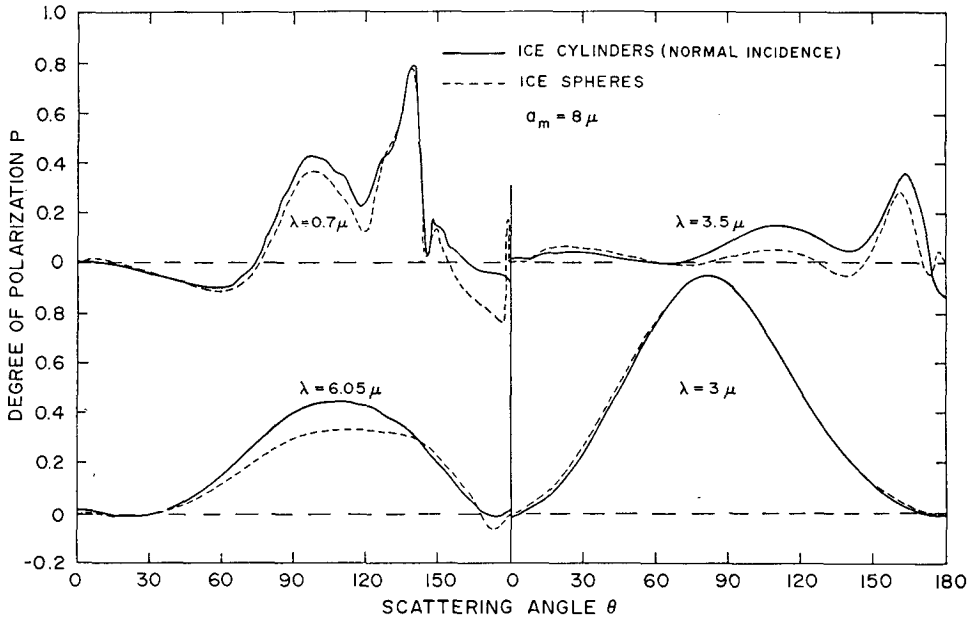

FIG. 5. Degree of polarization for uniformly oriented ice cylinders at normal incidence and for ice spheres. The horizontal dotted lines denote zero polarization. All the parameters are the same as in Fig. 4.

radius a_m. It should be noted that uniformly oriented cylinders may scarcely occur in the natural ice clouds. However, from a theoretical point of view, since this model produces scattering features similar to spheres, it is interesting to discuss briefly the significance of the results.

1) NORMAL INCIDENCE

The solid curves in Fig. 4 represent the phase functions for a sample of ice cylinders uniformly oriented in a horizontal plane at normal incidence, while the dotted curves denote those for the polydisperse ice spheres at wavelengths of 0.7, 3, 3.5 and 6.05 μ. The refractive indices for ice at these wavelengths were taken from the values tabulated by Irvine and Pollack (1968). They are shown in Table 1 where the size parameter for each case is also presented. We have used a mode radius of 8 μ throughout the computations. Since at normal incidence the rays penetrate the circular cross section of cylinders, we would expect that the scattering patterns of the cylinders should be similar to those of spheres. At $\lambda = 0.7\,\mu$, the primary cloudbow at the scattering angle of $\sim 135°$ is clearly shown for both cylinders and spheres. This feature arises from rays internally reflected once. The glory, however, disappears in the case of scattering by ice cylinders. The reason that spheres produce a glory at an inex of refraction outside the regions of $2\frac{1}{2}-2$ is because of the backscattering from edge rays which apparently are associated with the surface waves generated on the sphere. This phenomenon, which cannot be explained by means of geometrical optics, has been discussed by van de Hulst (1957), Bryant and Cox (1966), and Fahlen and Bryant (1968) for water drops. After comparison of the results for ice cylinders and spheres at this visible wavelength, we found that ice cylinders scatter more light in the regions near the scattering angle of $\sim 90°$ at the expense of scattering in the forward and backward directions. At $\lambda = 3.5\,\mu$, the primary cloudbows can still be observed for both ice spheres and cylinders, but their positions shift to larger scattering angles of $\sim 170°$ and $\sim 160°$, respectively. At $\lambda = 6.05\,\mu$, most of the rays undergoing internal reflections are absorbed inside the cylinders (or spheres), and the intensity is therefore a result only by the diffracted, the twice refracted, and the externally reflected rays. Finally, at $\lambda = 3\,\mu$, the absorption is so large that all the rays refracted into the particles are absorbed. Thus, the contributions to the intensity mainly come from diffraction and Fresnel reflection only. Generally speaking, ice spheres as compared with ice cylinders scatter more light in the regions where the scattering angles are less than 30°.

TABLE 1. Real (n_r) and imaginary (n_i) parts of refractive indices for ice, and mode size parameters (x_m) for $a_m = 8\,\mu$.

λ (μ)	n_r	n_i	x_m
0.7	1.31	0.0	71.81
3.0	1.13	0.2273	16.76
3.5	1.422	0.0163	14.36
6.05	1.235	0.0647	8.31

Fig. 5 illustrates the corresponding degree of linear

polarization for both ice cylinders and spheres [see Eq. (20)]. In addition to the information provided by the phase function, we note the following: At $\lambda=0.7\,\mu$, the negative polarization from the scattering angles of about 20°–75° arises from rays undergoing two refractions. The maximum polarization (~40%) at the scattering angle of ~90° is primarily due to the rays externally reflected on the surface of a cylinder or a sphere. The secondary cloudbow can also be seen, although it is not clear, at the scattering angle of ~120°. The polarization for the primary cloudbow is about 80% for both ice spheres and cylinders. The supernumerary bow of the primary cloudbow shown at the scattering angle of ~145° is the interference phenomenon (van de Hulst, 1957) which does not show in the phase function. At $\lambda=3\,\mu$, the noticeable positive polarization (~97%) at the scattering angle of ~80° is the result of Fresnel external reflection, although it contains a very small amount of energy. The interesting but not surprising results are that, for an incident unpolarized light, the positive polarization at 3.5 and 6.05 μ and a negative polarization at 3 μ are found at forward scattering ($\theta=0°$) for ice cylinders. Generally, from Figs. 4 and 5, we find better agreement in values of polarization than intensity for light scattered by uniformly oriented ice cylinders at normal incidence, and that by polydisperse ice spheres. Furthermore, polarization contains more pronounced features which could be valuable physical quantities for the identification of particle sizes.

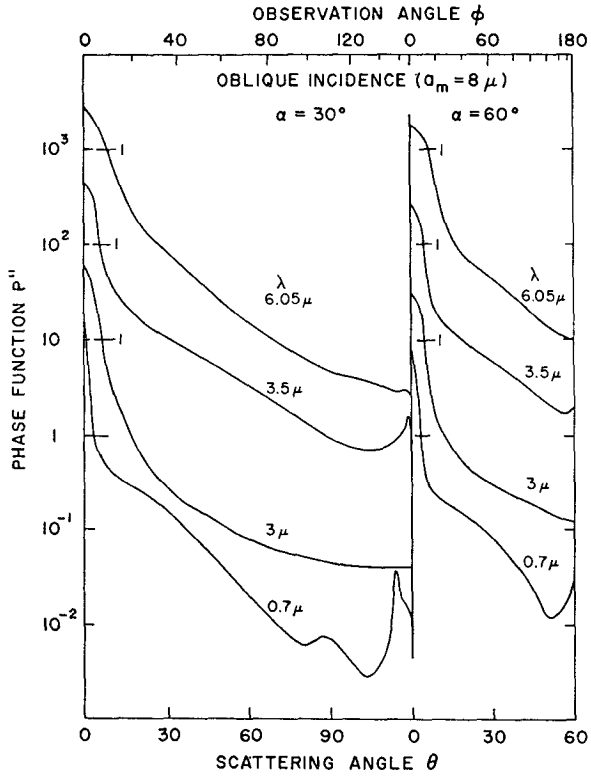

FIG. 6. Phase functions for uniformly oriented ice cylinders at oblique incidence for incident angles of 30° and 60°. The vertical scale applies to the lower-most curves. The scale for other curves can be obtained by dividing by a factor of 10 such that the horizontal bar on each curve occurs at unity. The horizontal scales at the bottom and the top are for the scattering and observation angles, respectively.

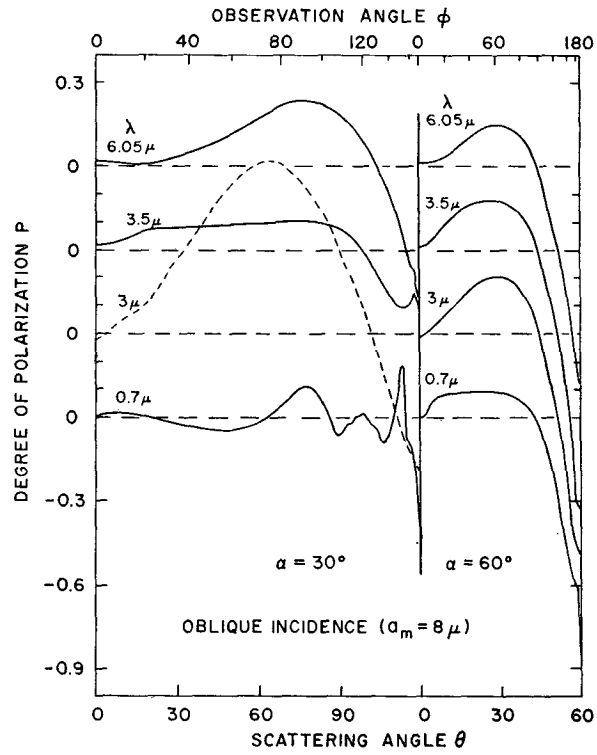

FIG. 7. Degree of polarization for uniformly oriented ice cylinders at oblique incidence. The horizontal dotted lines represent zero polarization. All the parameters are the same as in Fig. 6.

2) OBLIQUE INCIDENCE

Fig. 6 illustrates the results of phase functions for two cases of oblique incidence, $\alpha=30°$ and $\alpha=60°$. The lower scale is for the scattering angles which are linear, while the upper scale is for the corresponding observation angles according to Eq. (2). The other physical parameters employed in this section are exactly the same as in the last section. For $\alpha=30°$, the scattering angle varies from 0° to 120° due to geometry. At $\lambda=0.7\,\mu$, the two maxima shown at scattering angles of ~110° and ~90° seem to be caused by the skew rays internally reflected once and twice, respectively, analogous to the case of normal incidence. Similarly, at $\lambda=3.5\,\mu$, the maximum at the scattering angle of ~118° probably arises from rays undergoing one internal reflection. When $\alpha=60°$, the scattering angle does not exceed 60°. The scattering patterns for all four wavelengths become rather simple. We have also examined the results by increasing the oblique incident angle to 85° and have found that the angular scattering

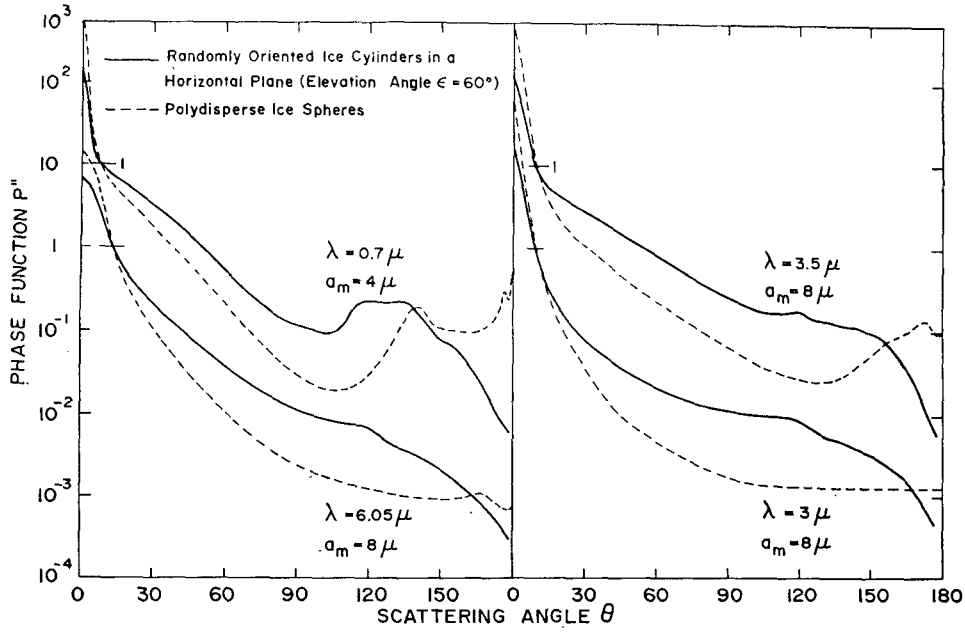

FIG. 8. Phase functions for randomly oriented ice cylinders in a horizontal plane (solid lines) and polydisperse ice spheres (dotted lines). The mode radius at an incident wavelength of 0.7 μ is 4 μ, while at incident wavelengths of 3, 3.5 and 6.05 μ it is 8 μ. The elevation angle is 60°. The vertical scale applies to the lower curves, while the scale for the upper curves can be obtained by dividing by a factor of 10.

patterns are very similar to those of isotropic scattering. Since very limited information is provided, we therefore did not present the results here.

Fig. 7 illustrates the degree of linear polarization in which the dotted lines represent zero polarization. Besides the features shown in the phase functions, there are also maxima due to externally reflected rays. In general, it appears that by increasing the oblique incident angle the positive polarization is reduced.

c. Randomly oriented ice cylinders in a horizontal plane

The results of the phase function for a sample of ice cylinders which are randomly oriented in a horizontal plane are shown in Fig. 8 based on Eq. (18). The primary purpose of integrating over the size parameter is to average out the interference fluctuations in the light scattering patterns which occur for a monodisperse sample of particles. At $\lambda=0.7\,\mu$, we used a mode radius of $4\,\mu$ instead of $8\,\mu$ in order to save computer time. This change, however, does not affect the general conclusions presented here. All the computations were made at an elevation angle $\mathcal{E}$ of 60°, i.e., the incident rays form angles of 60° with the horizontal plane. The assumption of random orientation implies that any position of the cylinder in a horizontal plane is equally probable. Thus, at this elevation angle, the incident angle α ranges from 0° to 30° [see Eq. (2)]. The intensities scattered in the same directions are added by means of the integration method. A small maximum, shown at the scattering angle of 120° for all four cases, is essentially a result of the scattering geometry caused by the ray having an incident angle of 30°. Generally, we found that cylinders scatter much more light compared to spheres in the region of scattering angles from ~20°–150°. Physically, this is caused by the large contributions from the depolarized components of the scattered electric field vector either perpendicular or parallel to the scattering plane at scattering angles other than those at the very forward directions. (The incident unpolarized light can be regarded as a superposition of two electric field vectors equal in magnitude but orthogonal in direction and with the same phase.)

Since the only contribution for direct backscattering is from rays incident normally on the cylinder, and since such positions at which rays can be incident perpendicularly upon it are very few in a random sample of cylinders, backscattering ($\theta\approx180°$) from long cylinders appears to be very small. It should be noted that small backscattering is also a result of the assumption that the length of the cylinder is much larger than its diameter. Most of the phase functions' features are washed out after integrating over all possible positions of cylinders in a horizontal plane, except at $\lambda=0.7\,\mu$, where the phase function has a maximum ranging from scattering angles of ~110°–135°.

At $\mathcal{E}=90°$, the incident rays are all normal to the cylinders no matter how they are oriented in the horizontal plane; the results, therefore, become the same as those of normal incidence obtained previously. This fact provides us with a physical as well as numerical checks on the computations.

We have also computed the phase functions for

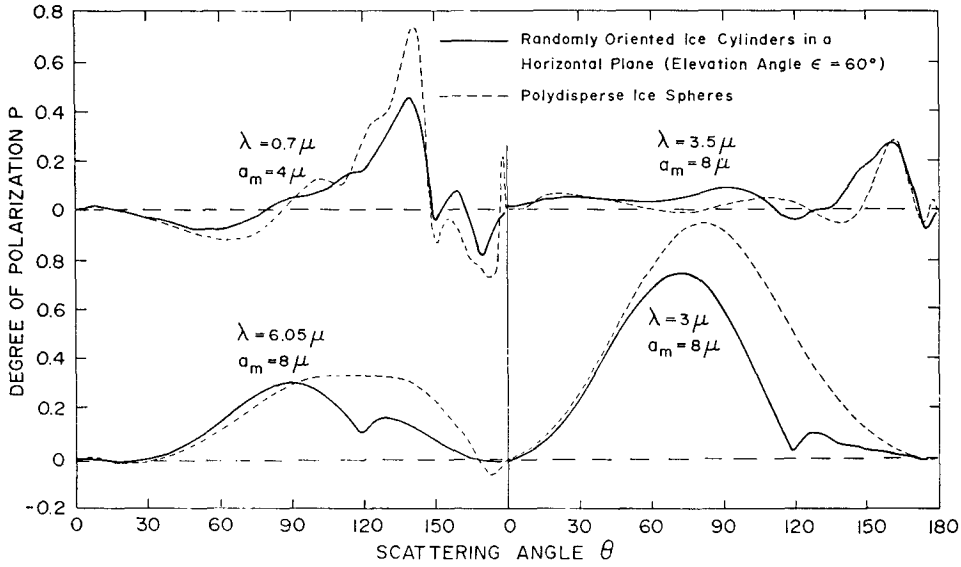

FIG. 9. Degree of polarization for randomly oriented ice cylinders in a horizontal plane (solid lines) and polydisperse ice spheres (dotted lines). The horizontal dotted lines represent zero polarization. All the parameters are the same as in Fig. 8.

elevation angles of 0°, 30° and 45°, and have found that the variations are not very significant. Hence, we would expect that results from random orientation in a plane or in a three-dimensional space should not differ significantly. Moreover, we can qualitatively extend our results if we recognize that hexagonal, as well as circular, cylinders whose lengths are again much larger than their diameters fall with their long axes parallel to the ground. Due to the variations in lengths and widths, they tend toward random orientation in a horizontal plane. As a result of randomness with respect to their long axes, it follows that light scattered by a sample of hexagonal cylinders should be very similar to that scattered by circular cylinders. The main discrepancy, however, would be that the circular cylinders cannot produce a halo which is one of the most beautiful and observable optical phenomenon from ice clouds. The halo phenomenon arises from the optical rays which undergo two refractions in a prism. For hexagonal cylinders, the position of the halo is 22° if the rays are normally incident on the cylinders (see, e.g., Humphreys, 1964). With skew rays, however, the position of the halo moves to larger scattering angles. The maximum value of the incident angle α for skew rays which can still produce halo is $\sim$60°, assuming an index of refraction of 1.31.

From the results obtained in this section, we must conclude that, compared to spheres, long cylinders randomly oriented in a plane scatter more light in the region of scattering angles from $\sim$20°–150° at the expense of scattering in both forward and backward directions.

Fig. 9 illustrates the corresponding degree of linear polarization at four different wavelengths. At the scattering angle of 120°, we noted before that the intensities have a slight maximum as a consequence of scattering geometry. This small maximum reduced the values of the positive polarization, particularly shown at 6.05 and 3 μ where the external reflections dominate the light scattering event. At $\lambda=0.7\,\mu$, the pronounced positive polarization ($\sim$80%) of cloudbows which arises from scattering by ice spheres (or ice cylinders at normal incidence) is greatly reduced for a sample of randomly oriented ice cylinders in a plane. The maximum is now only $\sim$40% and has become broader. This maximum comes from the rays normally or near normally incident on the cylinders. At $\lambda=3.5\,\mu$, the reduction of the feature at the scattering angle of $\sim$160° is not so large, but the maximum has indeed become broader.

While cylinders have two dimensions which are the same as spheres, they are nevertheless one kind of non-spherical particle. From the computations conducted in this study, we did obtain at least some information as to how scattering by non-spherical particles deviates from that by spheres. One such point was that features such as the cloudbows produced by scattering by spheres in the visible or near visible region would be distorted or at least be greatly reduced for non-spherical particles. Perhaps for irregular crystals these features would be completely lost. The glory, as discussed before, is absent in the case of scattering by ice cylinders and presumably will also disappear for irregular particles. Hence, measurements of linear polarization in the visible or near IR at positions around cloudbows or glory could be used for differentiation between cloud particles in the liquid or ice phase. Furthermore, Hansen (1971) has shown that multiple scattering from water clouds

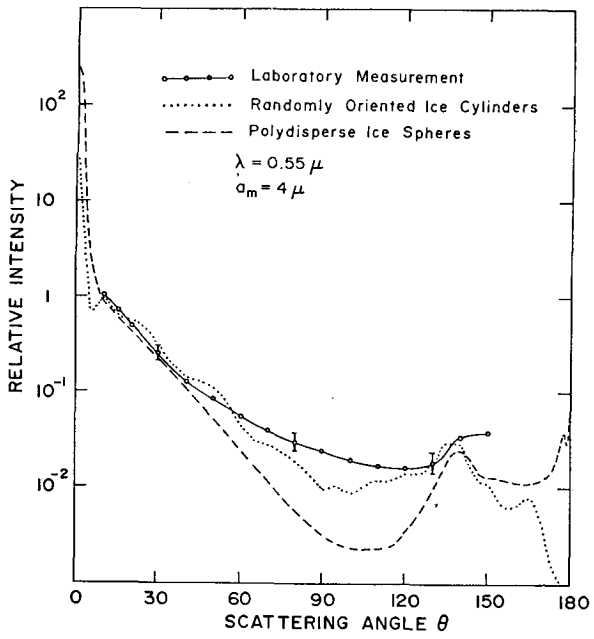

FIG. 10. Comparisons of the scattered intensity between the theoretical calculations for randomly oriented ice cylinders in a three-dimensional space (black dots) and the laboratory measurements for hexagonal columns made by Huffman and Thursby (solid line with circles). The dotted line is for polydisperse ice spheres having a mode radius a_m of 4 μ. The scattered intensities are all normalized to unity at the scattering angle of 10°. The incident light is unpolarized with a wavelength of 0.55 μ.

does not wash out polarization features because it arises from photons scattered once or a small number of times. His results emphasize the usefulness of polarization data.

d. Comparison of theory with laboratory measurement

Several laboratory experiments have been performed to investigate the angular scattering behavior of non-spherical particles. Holland and Draper (1967) and Holland and Gagne (1970) measured the scattered phase elements for a sample of irregular aerosols. Huffman and Thursby (1969) ahd Huffman (1970) used nephelometers to measure the angular scattering patterns (10°–150°) from artificial cirrus clouds created in a large laboratory cold chamber. For the purpose of comparison we employed the work by Huffman and Thursby on hexagonal columns, created at a temperature of −30C, which had a nearly log-normal distribution with a mode diameter (length of the columns) of 25 μ. The incident light was unpolarized at a wavelength of 0.55 μ.

The solid line with circles in Fig. 10 is the curve for the laboratory measurements, the vertical bars each indicating one standard deviation in the measured data. The dotted line represents the scattering pattern for polydisperse ice spheres having a Gamma distribution with a mode radius of 4 μ. Since the hexagonal columns obtained in the test chamber are probably in complete random orientation arising from air turbulence, we have extended the light scattering computation for monodisperse[1] circular cylinders with radii a of 4 μ which are randomly oriented in a three-dimensional space. The calculation for the phase function is as follows:

$$P^{11}(\theta) \propto \int_0^{\pi/2} \int_0^{\pi} i^{11}(\theta,\mathcal{E},\gamma) d\mathcal{E} d\gamma, \qquad (23)$$

where all the parameters have been defined earlier. The results are shown as black dots. The two theoretical curves in Fig. 10 are all normalized to unity at the scattering angle of 10° so that they may be compared with the values obtained by Huffman and Thursby. (It should be noted that they have pointed out that the crystal shapes and size distributions are not an important factor for light scattering measurements at scattering angles $<130°$.) In view of the uncertainty of the measurements, the theoretical calculations for randomly oriented ice cylinders appear to agree fairly well in the region of scattering angles from 10°–140°. Unfortunately, since the measurements were made only up to a scattering angle of 150°, we cannot predict the accuracy of the calculations for scattering in backward directions. The small discrepancy shown at the scattering angle of ~90° is probably due to the effects of scattering by small columns created in the cloud chamber. These small particles scatter much more light at scattering angles of ~90° at the expense of the forward scattering. The maximum beginning at the scattering angle of ~130° is similar to the primary cloudbow produced by spheres.

The polydisperse ice spheres appear to scatter much less light in the region from ~40°–130° scattering angles when compared with the values from laboratory measurements and those from randomly oriented ice cylinders. The largest difference is about one order of magnitude. It is unlikely that changing the size distribution for spheres will result in a better agreement in this region.[2] Furthermore, we have consistently found that the diffraction peak for randomly oriented long cylinders is much less than that for spheres, although it has been argued that the forward diffraction lobe from an assembly of non-spherical particles in random orientation would not be expected to differ much from that for an assembly of spheres (Hodkinson, 1963).

5. Conclusions and further recommendations

In this study, we have carried out computations of intensity and linear polarization for single scattering

[1] In a limited amount of computer time, we have not been able to integrate over the particle size. However, integrating over the particle orientations washes out most of the rapidly oscillating maxima and minima due to scattering by a single particle.

[2] J. E. Hansen and the author have made extensive Mie computations (unpublished) with several size distributions (power law, Gamma function, log-normal, and bimodal) having the same mean radius. We have found that such size distributions have insignificant effects on scattering properties.

by a sample of ice cylinders which are assumed to be either uniformly or randomly oriented in a horizontal plane. The calculations were made at wavelengths of 0.7, 3, 3.5 and 6.05 μ. It is found, compared to ice spheres, that ice cylinders generally scatter more light in regions near the scattering angle of $\sim 90°$ at the expense of scattering in the forward as well as backward directions. The cloudbows and glory produced by the scattering of spheres are either absent (glory) or greatly distorted and reduced (cloudbows) in the case of cylinders. Backscattering from long cylinders is found to be much less than that from spheres. Since a cylinder is one kind of non-spherical particle, the results reveal some information regarding the effect of non-sphericity on the scattering properties.

At present, we can conclude that the features such as the glory and cloudbows would be lost or at least be largely distorted for scattering by non-spherical scatterers. By utilizing this information, it is possible to discriminate between the liquid and ice phases of cloud particles, since ice clouds primarily contain non-spherical ice crystals, while water clouds consist of spherical water drops. Furthermore, since backscattering from randomly oriented long cylinders (such as needles, columns) are shown to be very small, it is also possible to distinguish these shapes from plates or irregular types of crystals which have strong backscattering returns.

We have made some comparisons of the angular scattering patterns between theoretical calculations and laboratory measurements and have found reasonably good agreement. The values of the computations carried out for randomly oriented ice cylinders should be applied with rather good accuracies to natural thin cirrus clouds because they contain predominantly hexagonal cylinders (Weickmann, 1945). Hence, the results of the angular and wavelength dependence of the scattered intensity may be used as basic quantities in problems of the evaluation of the transfer of visible or IR radiation through thick cirrus.

The study initiated in this paper represents *a first step in an attempt* to understand the scattered radiation by non-spherical particles. Further research can also be anticipated along the line of study presented here. The first step is to eliminate the assumption that cylinders are very long, so that the calculations can be performed for finite cylinders whose lengths may be comparable to, or smaller than, their diameters. Results in which the length of the cylinder is smaller than its diameter would be useful in the study of light scattering by plate-type crystals. Furthermore, the ray optics method, such as that used by Jacobowitz (1970) for infinite hexagonal cylinders, may also be valuable. However, the method should include the effects of polarization. This requires the transformation of the coordinates whenever the rays are refracted or reflected at the interface of the medium. Finally, along with theoretical investigations, carefully designed laboratory measurements similar to those conducted by Huffman and Thursby (1969) for scattering by ice crystals should also be undertaken. The precise measurements should be carried out so that accurate polarization data can be obtained. Moreover, the scattering measurements should also be made at scattering angles near 180°. These results would be very useful in the remote sensing of cloud particles, such as by means of radar or lidar backscattered return.

Acknowledgments. I would like to thank Dr. J. E. Hansen for reviewing this paper and for making several constructive suggestions. Discussions with Prof. R. M. Schotland and Dr. J. W. Hovenier are also acknowledged. During the course of this research, I held an NRC-NAS Research Associateship supported by NASA. I would also like to thank Dr. R. Jastrow for his hospitality at the Institute for Space Studies.

REFERENCES

Abramowitz, M., and I. A. Stegun, 1965: *Handbook of Mathematical Functions*. New York, Dover, 1046 pp.

Battan, L. J., 1959: *Radar Meteorology*. The University of Chicago Press, 161 pp.

Bryant, H. C., and A. J. Cox, 1966: Mie theory and the glory. *J. Opt. Soc. Amer.*, **56**, 1527–1532.

Cooke, D. D., and M. Kerker, 1969: Light scattering from long thin glass cylinders at oblique incidence. *J. Opt. Soc. Amer.*, **59**, 43–48.

Dave, J. V., 1969: Effect of coarseness of the integration increment on the calculation of the radiation scattered by polydispersed aerosols. *Appl. Opt.*, **8**, 1161–1167.

Deirmendjian, D., 1964: Scattering and polarization properties of water clouds and hazes in the visible and infrared. *Appl. Opt.*, **3**, 187–196.

——, 1969: *Electromagnetic Scattering on Spherical Polydispersions*. New York, Elsevier, 290 pp.

Fahlen, T. S., and H. C. Bryant, 1968: Optical backscattering from single water droplets. *J. Opt. Soc. Amer.*, **58**, 304–310.

Gary, G. A., and P. D. Craven, 1970: A note on the scattering geometry from infinite cylinders. *Appl. Opt.*, **9**, 2787–2788.

Hansen, J. E., 1971: Multiple scattering of polarized light in planetary atmospheres. Part II: Sunlight reflected by terrestrial water clouds. *J. Atmos. Sci.*, **28**, 1400–1426.

——, and J. B. Pollack, 1970: Near infrared light scattering by terrestrial clouds. *J. Atmos. Sci.*, **27**, 265–281.

Harris, F. S., Jr., 1971: Water and ice cloud discrimination by laser beam scattering. *Appl. Opt.*, **10**, 732–737.

Hodkinson, J. R., 1963: Light scattering and extinction by irregular particles larger than the wavelength. *Interdisciplinary Conf. Electromagnetic Scattering*, New York, Macmillan, 592 pp.

Holland, A. C., and J. S. Draper, 1967: Analytical and experimental investigation of light scattering from polydispersions of Mie particles. *Appl. Opt.*, **6**, 511–518.

——, and G. Gagne, 1970: The scattering of polarized light by polydisperse system of irregular particles. *Appl. Opt.*, **9**, 1113–1121.

Houghton, J. T., and G. E. Hunt, 1971: The detection of ice clouds from remote measurements of their emission in the far infrared. *Quart. J. Roy. Meteor. Soc.*, **97**, 1–17.

Huffman, P., 1970: Polarization of light scattered by ice crystals. *J. Atmos. Sci.*, **27**, 1207–1208.

——, and W. R. Thursby, Jr., 1969: Light scattering by ice crystals. *J. Atmos. Sci.*, **26**, 1073–1077.

Humphreys, W. J., 1964: *Physics of the Air*. New York, Dover, 676 pp.

Irvine, W. M., and J. B. Pollack, 1968: Infrared optical properties of water and ice spheres. *Icarus*, **8**, 324–366.

Jacobowitz, H., 1970: Emission, scattering and absorption of radiation in cirrus cloud layers. Ph.D. thesis, Dept. of Meteorology, M.I.T., 181 pp.

——, 1971: A method for computing the transfer of solar radiation through clouds of hexagonal ice crystals. *J. Quant. Spectry. Radiative Transfer*, **11**, 691–695.

Jayaweera, D. O., and B. J. Mason, 1965: The behavior of freely falling cylinders and cones in a viscous fluid. *J. Fluid Mech.*, **22**, 709–720.

Kerker, M., 1969: *The Scattering of Light and Other Electromagnetic Radiation*. New York, Academic Press, 666 pp.

Liou, K. N., 1972: Electromagnetic scattering by arbitrarily oriented ice cylinders. *Appl. Opt.*, **11** (in press).

——, and J. E. Hansen, 1971: Intensity and polarization for single scattering by polydisperse spheres: A comparison of ray optics and Mie theory. *J. Atmos. Sci.*, **28**, 995–1004.

——, and R. M. Schotland, 1971: Multiple backscattering and depolarization from water clouds for a pulsed lidar system. *J. Atmos. Sci.*, **28**, 772–784.

Mie, G., 1908: Beigrade für Optik trufen Medien speziell kolloidaler Metallosungen. *Ann. Phys.*, **25**, 377–445.

Ono, A., 1969: The shape and riming properties of ice crystals in natural clouds. *J. Atmos. Sci.*, **26**, 138–147.

Plass, G. N., and G. W. Kattawar, 1971: Radiative transfer in water and ice clouds in the visible and infrared region. *Appl. Opt.*, **10**, 738–748.

Lord Rayleigh, 1918: The dispersal of light by a dielectric cylinder. *Phil. Mag.*, **36**, 365–376.

Twomey, S., 1971: Radiative transfer: Terrestrial clouds. *J. Quant. Spectry. Radiative Transfer*, **11**, 779–783.

van de Hulst, H. C., 1957: *Light Scattering by Small Particles*. New York, Wiley, 470 pp.

Wait, J. R., 1955: Scattering of a plane wave from a circular dielectric cylinder at oblique incidence. *Can. J. Phys.*, **33**, 189–195.

Weickmann, H. K., 1945: Forman and Bildung atmospharischer Eiskristalle. *Beitr. Phys. Atmos.*, **28**, 12–52.